Accepted Manuscript

This is a post-peer-review, pre-copyedit version of an article published in International Journal of Environmental Science and Technology by Springer. The final authenticated version is available online at:
http://dx.doi.org/10.1007/s13762-017-1559-9

Tomaszewska, J., Smektała, P., Zgłobicka, I. et al. Int. J. Environ. Sci. Technol. (2018) 15: 1831.

Non-woven polypropylene fabric modified with carbon nanotubes and decorated with nano-akaganeite for arsenite removal

J. Tomaszewska[1,2], P. Smektała[1], I. Zgłobicka[1], J. Michalski[1], K. J. Kurzydłowski[1], Paweł Krzemiński,[3] C. Escudero-Oñate[3*]

[1] Faculty of Materials Science and Engineering, Warsaw University of Technology, Wołoska 141, 02-507 Warsaw, Poland
[2] Building Research Institute, Ksawerów 21, 02-656 Warsaw, Poland
[3] Norwegian Institute for Water Research (NIVA), Gaustadalléen 21, 0349 Oslo, Norway

* corresponding author: C. Escudero-Oñate
carlos.escudero@niva.no

Abstract

Due to its harmful impact on human health, presence of heavy metals, metalloids and other toxic pollutants in drinking or irrigation water is a major concern. Recent studies have proven that nanosized adsorbents are significantly more effective than their microsized counterparts. Particular attention has been given to nanocomposites with nanoadsorbents embedded in matrixes that could provide stability to the material and contribute to eliminating problems that may appear when using conventional granular systems.
This study presents the preparation of a novel hybrid filter from a commercially available polypropylene (PP) non-woven fabric matrix modified with multiwall carbon nanotubes (MWCNT) and iron oxy(hydroxide) nanoparticles, and its use in the removal of As(III). A Box–Behnken statistical experiment design has been chosen to explore relevant variables affecting the filter performance: (i) As(III) concentration, (ii) pH and (iii) sorbent dose. From an As(III) concentration of 10 $mg \cdot L^{-1}$, at pH 6.5 and with a sorbent dose of 5 $g \cdot L^{-1}$, the PP filter modified with MWCNT removes 10% of the initial metalloid concentration, reaching a capacity of 0.27 $mg \cdot g^{-1}$. After modification with iron oxy(hydroxide), the performance of the material is largely enhanced. The filter, under the same conditions, removes 90% of the initial As(III) concentration, reaching a capacity almost 10 folds higher (2.54 $mg \cdot g^{-1}$).
This work demonstrates that the developed hybrid filter is effective towards the removal of As(III) in a wide range of pHs. A cubic regression model to compute the removal of the filter as a function of pH and sorbent dose is provided.

Keywords: hybrid filter; optimization; iron oxy(hydroxide); As(III) removal; adsorbent; Box–Behnken.

1. Introduction

Multiphase solid materials containing nanoscale components have become a hot research topic nowadays and received much attention due to benefits offered by these materials compared to their conventional counterparts and other classes of materials. Due to their nanoscale size, these materials exhibit unique physical and chemical properties such as large surface to volume ratio and high interfacial reactivity. Therefore, the use of nanocomponents has a significant influence on particular features of composites, including among others their chemical reactivity, electrical, thermal, magnetic and optical properties, thus simultaneously giving new opportunities for their wider application (Kim and Van der Bruggen 2010). In recent years, many studies have demonstrated the utility of nanotechnology to remove organic and inorganic contaminants present in water (Bhatia et al. 2017; Shokati Poursani et al. 2017). From the different combinations of nanoscale materials, that may yield a product with good sorptive and/or catalytic properties in a stable and processable matrix, nanocomposites seem to be a reliable, future-proof alternative for environmental applications (Ghasemzadeh et al. 2014; Narayan 2010; Qu et al. 2013).

Due to its high toxicity and bioaccumulative nature, arsenic (As) is considered one of the most harmful water pollutants (WHO 2008). In natural waters and near neutral pH conditions, arsenic might be mostly found in inorganic forms as As(III) (arsenious acid/dihydrogen arsenite; $H_3AsO_3/H_2AsO_3^-$) or As(V) dihydrogen/monohydrogen arsenate (H_2AsO_4-/$HAsO_4^{2-}$). As(V) is less toxic and mostly present in immobile mineral forms, whereas As(III) is more toxic and is mobilized into water and living cells (Abernathy et al. 1997). The maximum concentration of As in drinking water, recommended by WHO, should not exceed 10 $\mu g \cdot L^{-1}$, however findings show that long-term consumption of water with such low levels of As can lead to arsenicosis (chronic arsenic poisoning), a condition whose major symptoms include skin lesions, peripheral neuropathy, diabetes, cardiovascular diseases and cancer (WHO 2008). Arsenic enters the environment through inputs from natural processes (e.g. weathering, volcanic emission, soil erosion) as well as through anthropogenic inputs (e.g. mining, combustion of fossil fuels, industry and agriculture). Additionally, increasing environmental awareness coupled with more stringent regulation standards has triggered various parties to challenge themselves in seeking appropriate wastewater treatment technologies (Teh et al. 2016). The arsenic pollution issue is a concern for authorities in both, developed and developing countries (Mandal and Suzuki 2002; Smedley and Kinniburgh 2002). The probability of global groundwater contamination was investigated in details by Amini and coauthors (Amini et al. 2008).

Conventional processes for treatment of As polluted effluents includes techniques such as oxidation, phytoremediation, coagulation – flocculation, ion exchange, adsorption, membrane separation and electrokinetic separation. Among these, adsorption seems to be preferred due to its high good efficiency coupled to its relatively low installation and operating costs, making it an affordable solution for both, developed and developing countries (Holl 2010). Although sorption-based processes for As removal are commonly used, the problems observed in conventionally used granular bed systems such as significant pressure drops and risk of release of the polluted particles into the environment still need to be overcome (Hristovski et al. 2007; Sperlich et al. 2005)

In this study, the authors have developed a polypropylene non-woven fabric with fibers of diameter in the range of 0.2–30 μm (commonly used as a filtering medium in commercial deep bed filters) modified with functionalized MWCNT and then decorated with iron oxyhydroxide nanoparticles in form of akaganeite (β-FeOOH). The literature indicates that iron oxides and oxy(hydroxides) are excellent candidates for arsenic sorption from aqueous effluents (Escudero et al. 2009; Habuda-Stanić and Nujić 2015; Moradlou et al. 2016; Sayed and Burham 2017). Furthermore, the mass transfer properties might be significantly enhanced by a synergistic effect with carbon nanotubes, which are known to possess high specific surface area, are easy to modify by physico-chemical methods and exhibit good performance in the removal of organic and inorganic contaminants from water (Behzadi et al. 2017; Hu et al. 2014; Tawabini et al. 2011). Immobilizing the adsorbent on the surface of a fibrous structure (non-woven polypropylene, which is a promising medium for separation of nanoobjects) (Przekop and Gradoń 2008; Żywczyk et al. 2015), an attempt was made to develop a novel filtering material combining high capacities of solid particles retention and As ions adsorption, simultaneously preventing the risk of release of nanoparticles into the environment and excessive pressure drops when applied in a fixed bed.

The modification method of the polymeric non-woven fabric with MWCNT and nano-akaganeite was developed at Warsaw University of Technology (Faculty of Materials Science and Engineering) in 2014 within Polish-Swiss Research Program NANOSORP. The sorption studies and the data assessment were performed at the Institute for Water Research (NIVA) in the period April-May 2015.

2. Materials and methods

2.1. Materials and reagents

Polypropylene (PP) non-woven fabric with fiber diameter sizes ranging from 0.2 to 30 μm were supplied by Amazon Filters Ltd. Multiwall carbon nanotubes (MWCNT), manufactured by CNT CO., LTD (South Korea), were used after purification with concentrated nitric acid (68% HNO_3, POCH) according to the procedure described by Jamrozik and coauthors (Jamrozik et al. 2014). For synthesis of iron oxy(hydroxide) nanoparticles, iron(III) chloride hexahydrate ($FeCl_3 \cdot 6H_2O$, Chempur), urea (NH_2CONH_2, POCH) and distilled water prepared with HLP10p Hydrolab (Poland) were used. Acetone (C_3H_6O) and 1-propanol (C_3H_8O) from POCH (Poland) were utilized as a wetting agent and solvent of a MWCNT suspension.
The chemicals for batch As adsorption experiments were obtained from: Sigma–Aldrich (United States) or Merck (Germany). In the experiments, NaOH (purity 99%), HCl (37% solution) and $NaAsO_2$ (standard solution 0.05 M) were used. All solutions were made using ultrapure water (MilliQ Water). The stock solution of sodium hydroxide (NaOH) was made by dissolving 1 g of NaOH in 100 mL of MilliQ water. The stock solution of hydrochloric acid (HCl) was prepared by dissolving 1 mL of concentrated HCl in 100 mL of MilliQ water. These solutions (HCl and NaOH) were employed to adjust the initial pH of the As(III) solutions to the target values of our study (4.0, 6.5 and 9.0).
Stock solutions of As(III) were made by dissolving appropriate amounts of standard $NaAsO_2$ Sigma-Aldrich solution (United States) in ultrapure water (MilliQ Water).

2.2. Embedment of MWCNT

A circle-shaped sample of non-woven PP fabric (diameter – 65 mm, thickness – 1 mm) was mounted on a stainless steel frame and immersed in an ultrasonic bath (Codyson CD-4860) at a frequency of 35 kHz filled with 1-propanol suspension of MWCNT at concentration of 10 $mg \cdot L^{-1}$. After 10 minutes, the sample was taken out of the bath, drip-dried and placed in an oven heated to 130°C for 5 minutes. In order to obtain homogenous distribution of MWCNT onto the entire surface of fibres, this procedure was repeated 5 times. The product obtained was labelled as PP-MWCNT.

2.3. Decoration with iron oxy(hydroxide) nanoparticles

PP exhibits strong hydrophobic properties, therefore before the decoration with iron oxy(hydroxide), the non-woven fabric samples with embedded MWCNTs were wetted with acetone and washed in distilled water. Next, the samples were processed in a pressure reactor filled with 335 mL of aqueous solutions of 14 mM $FeCl_3$ and 40 mM $CO(NH_2)_2$ at the temperature of 100 ºC for 1 hour. Before proceeding to a further stage, the samples were washed with distilled water and dried at room temperature. The product obtained was labelled as PP-MWCNT-FeOOH.

2.4. Characterization of the adsorbent

The surface morphologies of the raw non-woven fabric and the MWCNT-modified non-woven fabric decorated with iron oxy(hydroxide) nanoparticles were observed using scanning electron microscopy (SEM, SU8000, Hitachi Ltd., Japan) in secondary electron (SE) imaging mode at 1 and 3 kV, respectively. X-ray diffraction (XRD) analysis was carried out using a Bruker 8D Advance X-ray diffractometer equipped with Cu K_α radiation (λ = 1,54Å), operating at 40kV and 10mA. The diffraction data were recorded for 2Θ values range of 25–70° with a step of 0.054° and time per step of 960 s. Phase identification was performed using PDF-2/Release 2010 RDB database. The infrared spectra of both, PP-MWCNT and PP-MWCNT-FeOOH has been recorded in the frequency range 500-4000 cm^{-1} using a step of 1 cm^{-1}. Spectra were processed using Omnic™ softwarer (ThermoFisher Scientific).

2.5. Batch mode adsorption experiments

The extent of As(III) removal was studied by exposing a given amount of adsorbent to 10 mL of As(III) solutions in stoppered plastic tubes. The solutions were kept under stirring at 300 rpm on a Titramax 101 vibrating platform shaker (Heidolph, Germany) for 24 h. Samples during agitation were also shaken individually at 1000 min^{-1} using a vortex shaker (IKA® Werke GmbH & Co. KG, Germany). After the exposure, the As(III) solutions were diluted with 5 mL of ultrapure water, shaken, and stored for further analysis.
The measurement of As(III) concentration in aqueous solutions was performed using an inductively coupled plasma-mass spectrometer (ICP-MS; Agilent 7700x) equipped with an octopole collision cell and an automatic sample introduction system (ASX–500 Series Autosampler). The limit of quantification (LOQ) of the ICP-MS optimized method was 0.025 μgL^{-1}.

2.6. Experimental design and statistical analysis

A Box–Behnken experimental design method was used to assess the effect of relevant operating parameters on As(III) removal and to establish their optimum combination. These variables are: pH, As(III) concentration and sorbent dose, labelled as X_1, X_2 and X_3, respectively. The pH range studied was from 4 to 9, the As(III) concentration from 500 to 10,000 μg·L^{-1} and the sorbent dose varied between 5–50 g·L^{-1}. The experimental design involved three parameters (X_1, X_2 and X_3), each at three levels, coded –1 (low), 0 (medium), and +1 (high). A summary of the aforementioned factors can be seen in Table 1.

Table 1. Levels of each factor employed in the Box–Behnken study of As(III) removal.

Independent factors	**Symbol**	**Coded levels**		
		–1	0	1
pH	X_1	4.0	6.5	9.0
Initial As concentration (μg·L^{-1})	X_2	500	5250	10000
Sorbent dose (g·L^{-1})	X_3	5.0	27.5	50.0

The summary of the conditions for the different experimental points of the Box–Behnken statistical design are shown in Table 2. The number of experiments N was calculated according to the equation:

$$N = k^2 + k + cp \quad (1)$$

where, k indicates a factor number and cp indicates the replicate number of the central point (Kousha et al. 2012). The obtained values were fitted using linear, quadratic and cubic model, with the last, cubic, yielding the best fitting. The central point of the experimental design was repeated five times to determine error. To correlate As removal efficiency (Y) with the independent variables explored (X_1–X_3), the next response surface function was employed:

$$Y = b_0 + b_1X_1 + b_2X_2 + b_3X_3 + b_{12}X_1X_2 + b_{13}X_1X_3 + b_{23}X_2X_3 + b_{11}X_1^2 + b_{22}X_2^2 + b_{33}X_3^2 + b_{123}X_1X_2X_3 + b_{112}X_1^2X_2 + b_{113}X_1^2X_3 + b_{122}X_1X_2^2 + b_{133}X_1X_3^2 + b_{223}X_2^2X_3 + b_{233}X_2X_3^2 + b_{111}X_1^3 + b_{222}X_2^3 + b_{333}X_3^3 \quad (2)$$

being, Y the predicted response (As removal %), b_0 – model constant, b_1–b_3 – linear coefficients, b_{12}, b_{13}, b_{23}, b_{123}, b_{112}, b_{112}, b_{122}, b_{133}, b_{223}, b_{233} – the cross product coefficients, b_{11}, b_{22}, b_{33} – quadratic coefficients and b_{111}, b_{222}, b_{333} – cubic coefficients.

Table 2. Experimental set of the Box–Behnken design for optimization of As(III) removal

Run	pH	Initial As concentration ($mg \cdot L^{-1}$)	Sorbent dose ($g \cdot L^{-1}$)
1	6.5	5.25	27.5
2	6.5	5.25	27.5
3	6.5	5.25	27.5
4	6.5	5.25	27.5
5	4.0	5.25	5.0
6	4.0	10.00	27.5
7	9.0	5.25	50.0
8	9.0	0.50	27.5
9	6.5	10.00	5.0
10	6.5	0.50	50.0
11	4.0	0.50	27.5
12	6.5	0.50	5.0
13	9.0	5.25	5.0
14	9.0	10.00	27.5
15	6.5	10.00	50.0
16	4.0	5.25	50.0
17	6.5	5.25	27.5

The Design Expert software (trial version 9.0.4.1, Stat–Ease Inc., Minneapolis, USA) was used in the experimental design as well as in the determination of the characteristic coefficients and the subsequent data analysis. The As(III) removal efficiency was examined for the two materials studied in the present work (PP-MWCNTs and PP-MWCNTs-FeOOH) characterized by two indicators: removal percentage (*R%,* Eq. (3)) and adsorbent capacity (q_t, Eq. (4)). The calculations were conducted through the equations:

$$R(\%) = (C_o - C_f)/C_o \cdot 100 \quad (3)$$

$$q = (C_o - C_f) \cdot V/m \quad (4)$$

where *R (%)* is removal percentage, q is the amount of As(III) taken up by the adsorbent ($\mu g \cdot g^{-1}$) and C_0 and C_f the initial and final As(III) concentrations in the solution respectively ($\mu g \cdot L^{-1}$). V and m indicate the volume of the solution (L) and the weight of the adsorbent (g) respectively.

3. Results and discussion

3.1. Characterization of hybrid filters

Scanning electron microscopy (SEM) images of the non-woven fabric before modification and after deposition of multiwall carbon nanotube (MWCNT) and decoration with iron oxy(hydroxide) are presented in Fig. 1 (a) and (b, c, d) – respectively. The images presented in b, c and d correspond to the same exploration point of the fiber at different magnifications. As it can be observed, the raw material (a) exhibits the characteristics entanglement of a plastic non-woven fabric. After modification with MWCNT and the iron oxy(hydroxide), the original flat and clean surface of the polypropylene fibers appears covered with a thin and fluffy material. Similar electronic pictures have been obtained by other authors when exploring the deposition of MWCNTs in non-woven fabrics (Sano and Akiba 2014). It can be inferred from the images that the ultrasonic treatment combined with heating approaching the melting point of PP resulted in a homogeneous distribution of MWCNTs on the fibers. The extremely homogeneous distribution of nanoparticles when using ultrasound-based procedures was also reported by Teh and co-authors (Teh et al. 2017) during the synthesis of photocatalysts. The decoration performed in a next step maximized the amount of iron oxy(hydroxide) nanoparticles in the filter by locating them on both the MWCNT and the non-woven fibers.

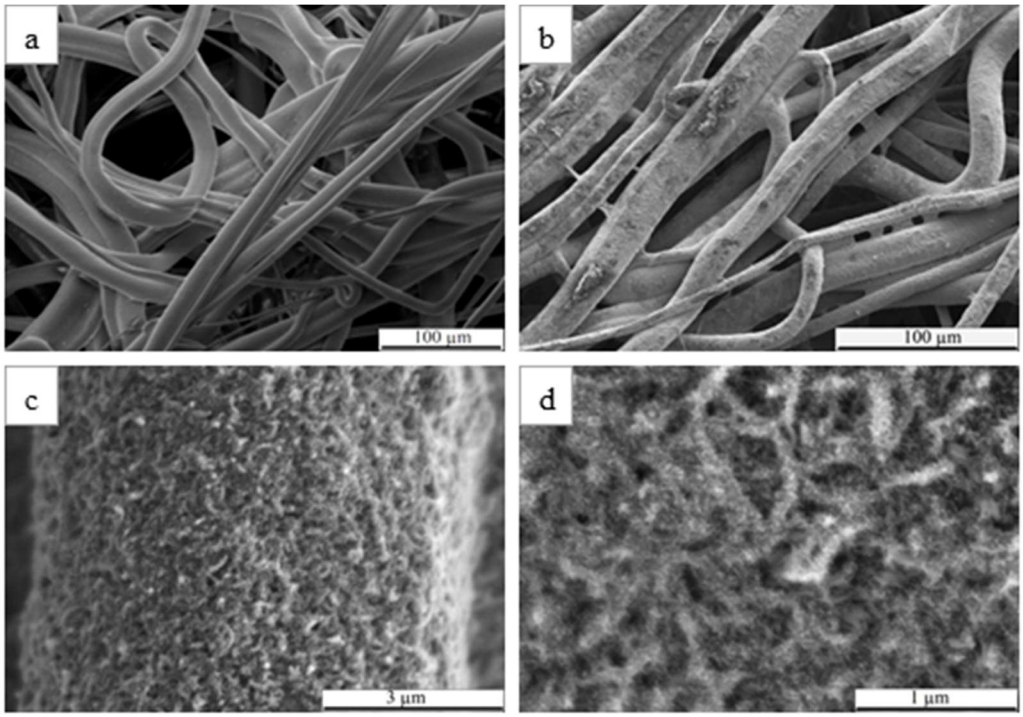

Fig. 1 SEM images of (a) unmodified non-woven fabric and (b, c, d) MWCNT-modified non-woven fabric decorated with iron oxy(hydroxide) nanoparticles.

The MWCNT-modified non-woven PP fabric decorated with iron oxy(hydroxide) nanoparticles were further characterized by X-Ray Diffraction (XRD). The diffractogram obtained is presented in the Figure 2. The characteristic diffractograms of alpha-polypropylene and of akaganeite are also included in the same figure. The match of the reflection peaks observed indicate that the iron oxy(hydroxide) phase is tetragonal akaganeite (β-FeOOH) and the broadening of its diffraction peaks points out that the material has a small particle size. The characteristic peaks of the MWCNT can hardly be identified from the pattern, possibly because being overlapped with other peaks.

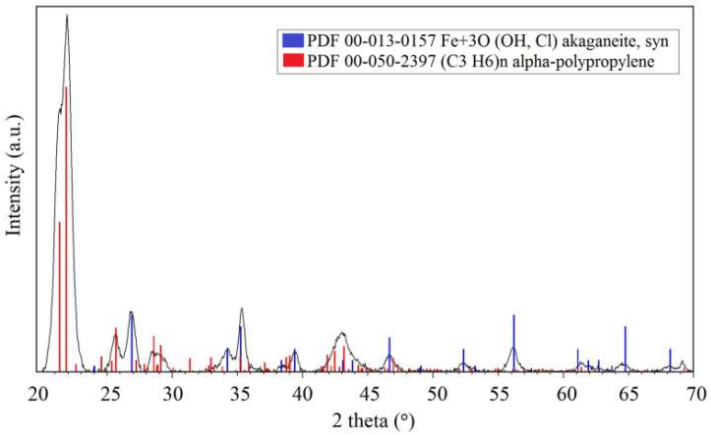

Fig. 2 The XRD pattern of MWCNT-modified non-woven PP fabric decorated with iron oxy(hydroxide).

The FTIR spectra were recorded in the range 500-4000 cm-1 for both, PP-MWCNT and for the same material after decoration with nano-akaganeite (PP-MWCNT-FeOOH). The characteristic spectra are presented in Figure 3.

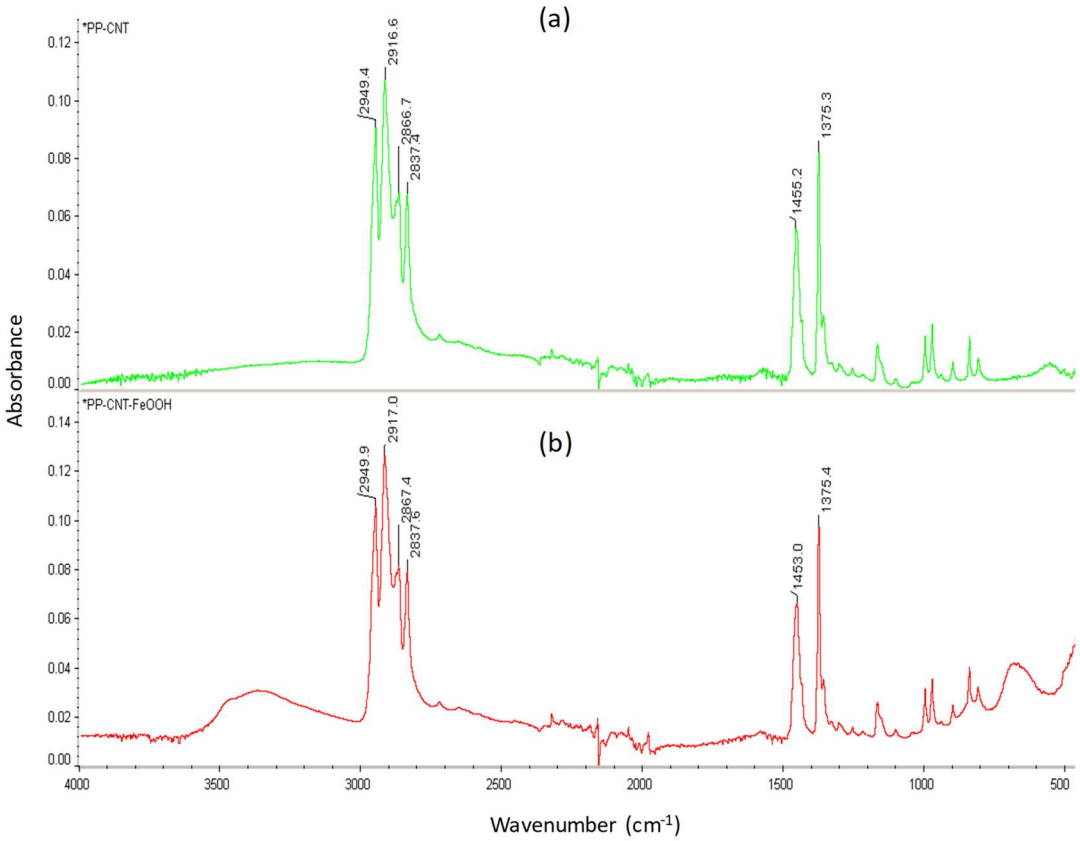

Fig. 3 FTIR spectra of (a) MWCNT-modified non-woven PP fabric and (b) decorated with iron oxy(hydroxide).

The FTIR spectra obtained from the PP-MWCNT allows mainly detecting the bands associated to the backbone of PP. These characteristic bands are located at 2949, 2917, 2867, 2837 cm^{-1} and correspond to the C–H stretching vibration of PP. The band appearing at about 1455 corresponds to the asymmetric $–CH_3$ and $–CH_2$ bending vibration of PP and that appearing at about 1375 is indicative of the symmetric $–CH_3$ bending vibration (Grant and Ward 1965).
In addition to the intense aforementioned bands, some others can be observed. This is the case of the bands band located at about 998, characteristic of the $–CH_3$ rocking vibration.
After deposition of the akaganeite in the filter matrix, the main modifications observed are the appearing of a large band centered at about 3350 cm^{-1}, corresponding to bulk -OH stretch and free surface -OH groups (Escudero et al. 2009). The band appearing at about 690 can be ascribed to the -OH bending in β-FeOOH (Bashir et al. 2009).

3.2. Adsorption experiments

The results of the experiments conducted for the three different pH values, three different initial As(III) concentrations and three different sorbent doses are listed in Table 3. The removal (%) and capacity results ($\mu g \cdot g^{-1}$) obtained in the different experiments are also presented in Table 3. The middle point (pH 6.5, initial As(III) concentration of 5250 $\mu g \cdot L^{-1}$ and sorbent dose of 27.5 $g \cdot L^{-1}$) was repeated five times in order to reduce measurement errors. As it can be observed, the divergence between the results obtained for the central point is negligibly small, proving high repeatability of the test. As observed, the filters containing FeOOH adsorb a larger amount of As(III) in all the conditions explored. The sorption of As(III) seems to be mostly dependent on the initial concentration and sorbent dose. The sorbate-sorbent systems are less sensitive to the initial pH of the solution in the range explored.

Table 3. Removal efficiency and adsorbent capacity of As(III) obtained for PP-MWCNT and PP-MWCNT-FeOOH in the different experiments

pH	Initial As concentration [µg·L^{-1}]	Sorbent dose [g·L^{-1}]	PP-MWCNT		PP-MWCNT-FeOOH	
			Removal [%]	q [µg·g^{-1}]	Removal [%]	q [µg·g^{-1}]
4.0	500	27.5	15	3.06	100	19.99
4.0	5250	5	20	279.40	43	568.18
4.0	5250	50	21	31.15	100	141.98
4.0	10000	27.5	48	226.96	98	475.14
6.5	500	5	16	15.97	98	99.55
6.5	500	50	13	1.45	100	10.91
6.5	5250	27.5	68	180.80	99	264.20
6.5	5250	27.5	72	191.04	100	264.86
6.5	5250	27.5	68	178.05	97	251.06
6.5	5250	27.5	69	179.35	100	264.78
6.5	5250	27.5	71	192.45	99	259.89
6.5	10000	5	10	270.67	90	2544.46
6.5	10000	50	83	211.86	100	246.03
9.0	500	27.5	n.d.	n.d.	100	20.03
9.0	5250	5	47	669.92	73	1013.43
9.0	5250	50	32	45.16	99	136.68
9.0	10000	27.5	62	291.63	98	461.22

n.d. – not determined

The response coefficients (Eq. (2)) for As(III) removal were obtained using the experimental dataset and a cubic response function. The results are presented in Table 4. A comparison between the experimental and predicted As(III) removal (%) for modified sorbent polypropylene non-woven and the same material decorated with FeOOH has been performed. The results are presented in Figure 4 (a) and (b) respectively.

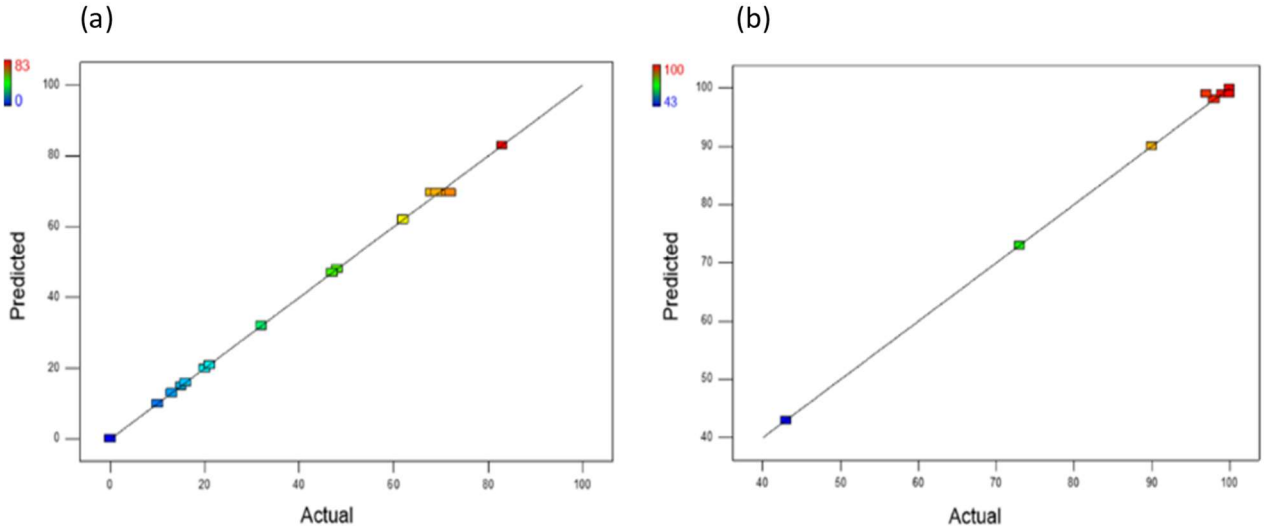

Fig. 4 Observed and predicted As(III) removal efficiency of (a) MWCNT-modified non-woven fabric (PP-MWCNT) and (b) of MWCNT-modified non-woven fabric decorated with iron oxy(hydroxide) nanoparticles (PP-MWCNT-FeOOH)

Table 4. Box–Behnken obtained coefficient for the cubic model

Coefficients	PP-MWCNT	PP-MWCNT-FeOOH
b_0	69.60	99.00
b_1	9.50	7.25
b_2	16.00	–2.00
b_3	17.50	3.00
b_{12}	7.25	0.00
b_{13}	–4.00	–7.75
b_{23}	19.00	2.00
b_{11}	–19.43	–9.13
b_{22}	–18.93	9.12
b_{33}	–20.18	–11.12
b_{123}	0.00	0.00
b_{112}	7.75	1.00
b_{113}	–21.00	17.75
b_{122}	–9.75	–7.25

As it can be observed, an excellent agreement between the experimental values and those predicted by the cubic response function was achieved for both materials. The correlation coefficients (R^2) achieved were 0.999 and 0.998 for PP-MWCNT and PP-MWCNT-FeOOH, respectively. It can be noticed that As(III) removal efficiencies varied from 0% to 83% for PP-MWCNT, and between 43% to 100% for PP-MWCNT-FeOOH.

An ANOVA statistical test was used to estimate the statistical significance of the model. The models were used for the construction of contour and three-dimensional response surface plots to predict the relationship between the independent variables and the removal of As(III). These plots are presented in Figure 5 and 6.

Table 5. Analysis of variance (ANOVA) of response surface cubic model for PP-MWCNT and PP-MWCNT-FeOOH

	PP -MWCNT	PP-MWCNT-FeOOH
p–value (Prob > F)	<0.0001	<0.0001
Std dev	1.82	1.22
C.V. %	4.32	1.31
R–squared	0.999	0.998
Adj R–squared	0.996	0.99
Adeq Precision	52.3	53.2

Table 5 shows the results of statistical analysis of the achieved data. The p-values are lower than 0.05 for all modified non-wovens, indicating then that the models are statistically significant. The adjusted R^2 value (close to 1) indicates the capability of the developed models to satisfactorily describe the system behavior within the range of operating factors (Shak and Wu 2015). Results can be considered significant if the coefficient of variation (C.V.) is not higher than 15% (Rossi 2010). Values lower than 15% were obtained for PP-MWCNT (4.32%) and PP-MWCNT-FeOOH (1.31%).

The Design Expert 9.0 was used to create 2D contour plots and a 3D response surface for As(III) removal efficiencies of the formed hybrid filters and three sorbent doses: 5 g·L^{-1}, 27.5 g·L^{-1} and 50 g·L^{-1}, respectively (Figure 4 and 5).

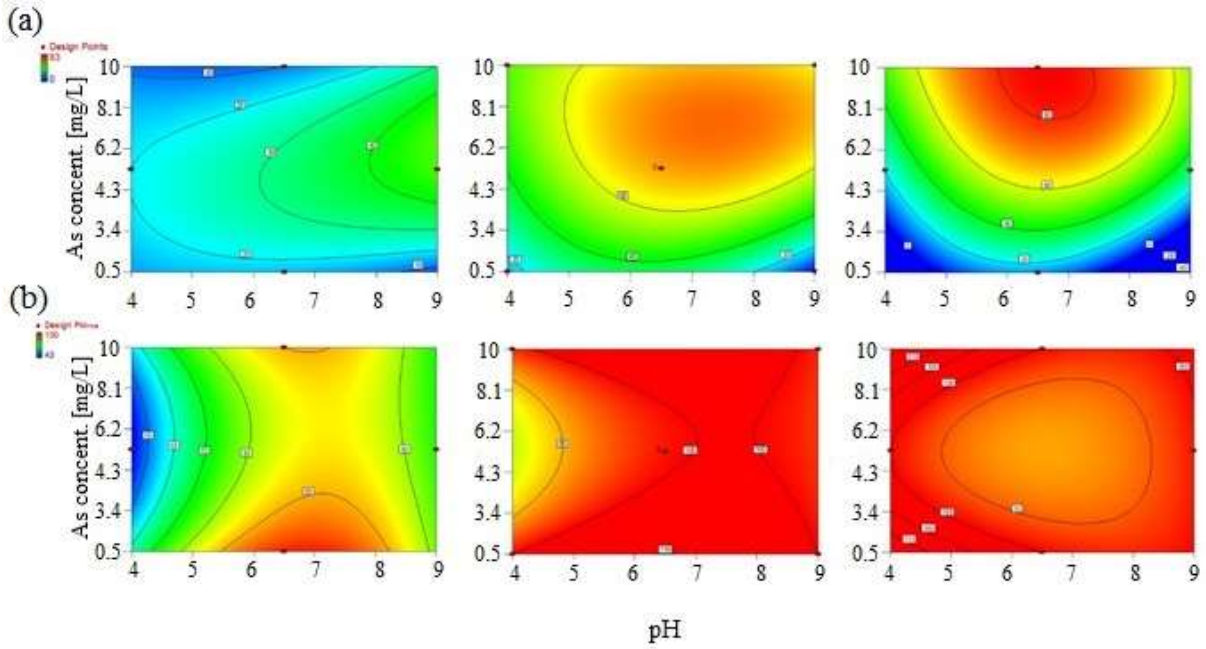

Fig. 5 Contour plots of As(III) removal efficiency of (a) PP-MWCNT for sorbent dose of 5 g·L^{-1}, 27.5 g·L^{-} and 50 g·L^{-1} (from left to right) and (b) PP-MWCNT-FeOOH for sorbent dose of 5 g·L^{-1}, 27.5 g·L^{-} and 50 g·L^{-1} (from left to right)

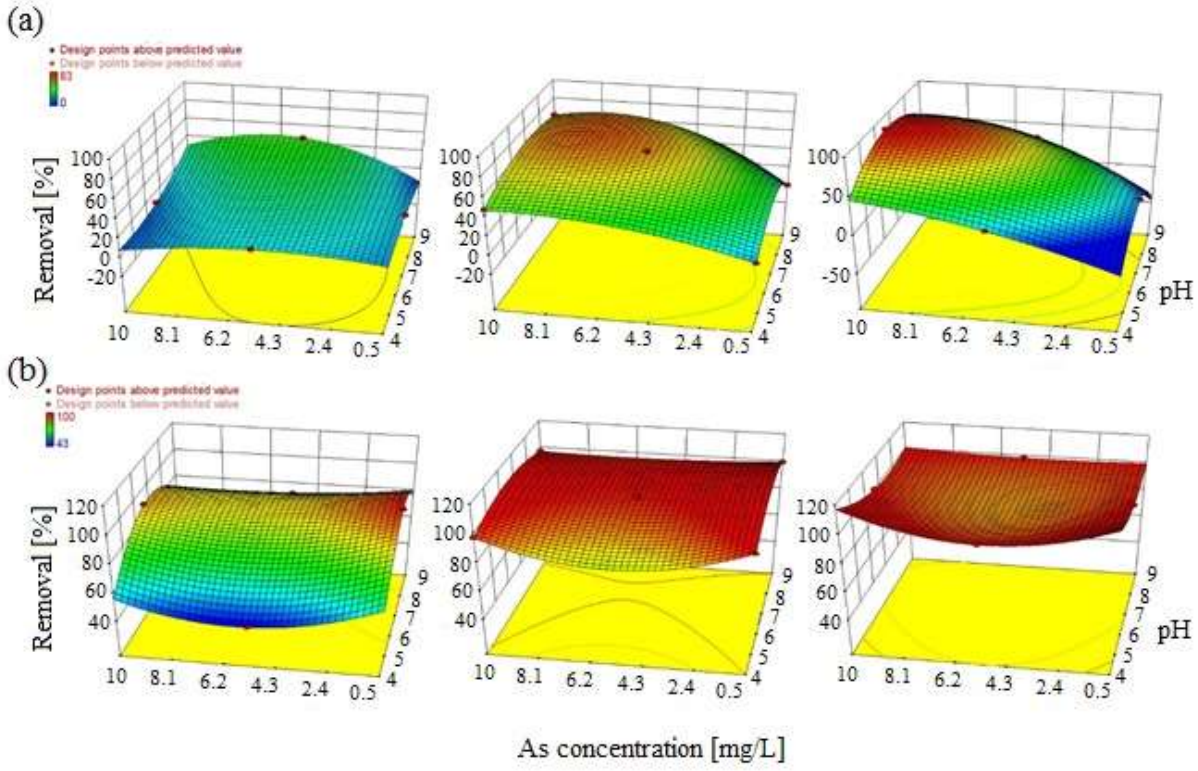

Fig. 6 Response surface plots of As(III) removal efficiency of (a) PP-MWCNT for sorbent dose of 5 g·L^{-1}, 27.5 g·L^{-} and 50 g·L^{-1} (from left to right) and (b) PP-MWCNT-FeOOH for sorbent dose of 5 g·L^{-1}, 27.5 g·L^{-} and 50 g·L^{-1} (from left to right)

Based on the obtained results, it can be concluded that the PP-MWCNT-FeOOH hybrid filter exhibits a much higher removal performance for As(III) compared to PP-MWCNT. PP-MWCNT filters have demonstrated the highest As(III) uptake (up to 83%) at pH 6.5, whereas PP-MWCNT-FeOOH removed up to 100% of As(III) ions almost regardless on pH levels in the system. The highest adsorption capacity (2.5 $mg \cdot g^{-1}$) for PP-MWCNT-FeOOH was achieved for an As(III) concentration of 10 $mg \cdot L^{-1}$, a sorbent dose of 5 $g \cdot L^{-1}$ and a pH 6.5. It is noteworthy that this adsorption capacity does not necessarily constitute the maximum adsorption capacity (q_{max}) of the hybrid filter. In order to estimate q_{max} of PP-MWCNT-FeOOH, further studies would be required.
In the literature on the topic, authors usually present q_{max} calculated for various adsorption models. Depending on the speciation and morphology of employed iron oxide or oxy(hydroxide) nanocomponents and manufacturing method, various functionalities and effectiveness of carbon-based nanocomposites toward As(III) ions have been demonstrated. A summary of the maximum capacities achieved by carbon nanotubes modified with different iron-based materials in the removal of As(III) is presented in the Table 6. For comparison sake, the results obtained by our filters are also included. As it might be observed, capacities of 1.72 and 4 $mg \cdot g^{-1}$ have been reported when using iron oxide-MWCNT. In the case of carbon nanotubes coated with magnetic iron oxide, authors have reported capacities of 8.13 and 20.17. In the case of magnetite-MWCNTs, authors have indicated a maximum As(III) capacity about 53 $mg \cdot g^{-1}$.

Table 6. Effectiveness of carbon-based nanocomposites toward As(III) ions adsorption

Nanosorbent	**pH**	**Q As(III) ($mg \cdot g^{-1}$)**	**Reference**
Polypropylene fabric with multiwalled carbon nanotubes decorated with iron oxy(hydroxide) (PP-MWCNT-FeOOH)	6.5	2.5	This study
Polypropylene fabric with multiwalled carbon nanotubes (PP-MWCNT)	6.5	0.27	This study
Iron oxide-multiwalled carbon nanotubes (Fe-MWCNT)	4	1.72	(Addo Ntim and Mitra 2011)
Iron oxide-multiwalled carbon nanotubes (Fe-MWCNT)	8	4.00	(Tawabini et al. 2011)
Magnetic iron oxide/carbon nanotubes (MI/CNTs)	N.A.	8.13	(Ma et al. 2013)
Magnetic iron oxide/carbon nanotubes (MIO-CNTs)	7	20.17	(Chen et al. 2014)
Magnetite multiwalled carbon nanotubes (Fe_3O_4-MWCNTs)	N.A.	53.15	(Mishra and Ramaprabhu 2010)

3.3. Sorption mechanism

For a proper discussion on potential sorption mechanisms, it becomes of paramount importance gathering information of the solid phase structure, but also knowing the species distribution of the sorbate (in our case, As(III)). Therefore, the hydrochemical speciation as a function of pH for As(III) in the range 2 to 12 for an initial concentration of 5.25 $mg \cdot L^{-1}$ has been simulated (Fig.7) , and a sorption mechanism has been proposed (Fig. 8).

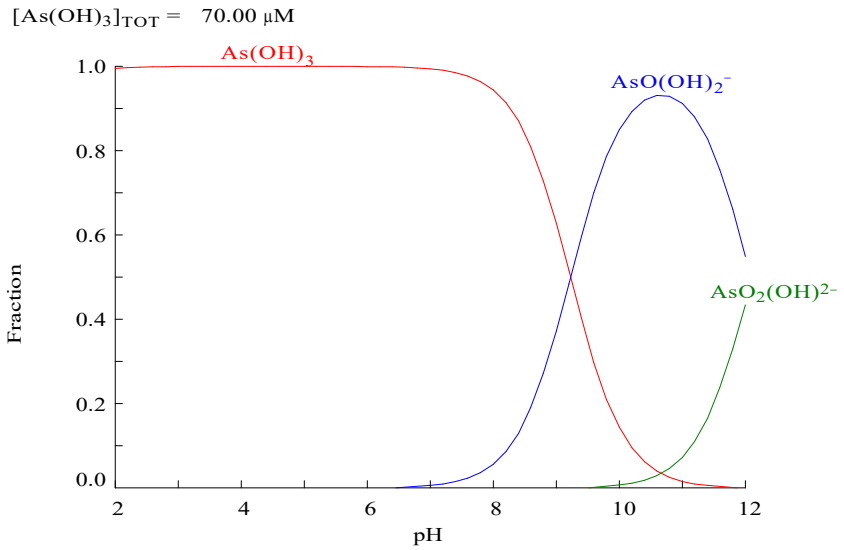

Fig. 7 Speciation of As(III) in water as a function of pH. Simulated initial concentration: 5.25 mg·L^{-1}.

The simulation results clearly demonstrate that As(III) remains as neutral arsenious acids (H_3AsO_3) in most of the pH range studied in our study. From pH 4 to approximately 8, almost all the arsenic present in solution exists as H_3AsO_3. Despite the formation of the monovalent dihydrogenarsenite $H_2AsO_3^-$ actually starts at pH 7, its concentration only exceeds 50% respect to the original As(III) concentration when pH exceeds 9.2 (pKa of the weak acid H_3AsO_3).

On the basis of the former discussion, the removal of arsenic by the sorbents developed in this work has to be tackled assuming that arsenic in solution occurs as the neutral species H_3AsO_3.

The sorption assays performed demonstrate that the raw, unmodified PP-MWNT has small capacity to adsorb As(III), despite in the optimum loading conditions (initial concentration: 5.25 mg·L^{-1}; pH: 9; sorbent dose: 5 g·L^{-1}), the material achieves a capacity of barely 0.67 mg·g^{-1}. The slight adsorption observed may be due to weak interactions, such as van der Waals forces, between the neutral H_3AsO_3 and the -OH present in the surface of the carbon nanotubes. Here it should be remarked that the raw CNTs were exposed to concentrated HNO_3, being therefore exposed for a potential oxidation of the surface (Rosca et al. 2005) that could have led to the inclusion of -OH groups.

The large enhancement of the capacity of the sorbent material when including FeOOH in the structure can be explained by the presence of the large amount of free hydroxyl groups of the metal oxy(hydroxide). As(III) species have a large affinity towards FeO-OH moieties, and the metalloid can be therefore adsorbed through complexation with oxy(hydroxide) sites on the sorbent surface according to the scheme presented:

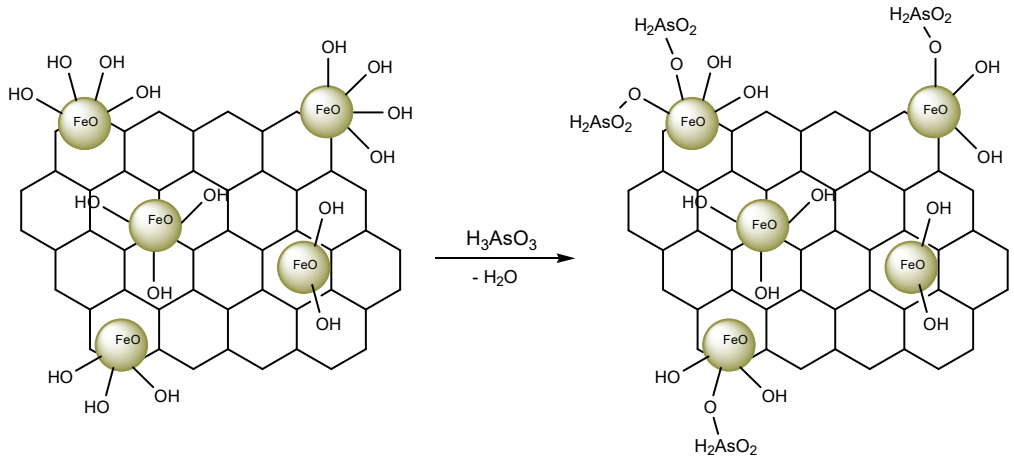

Fig. 8 Mechanism of As(III) removal by PP-MWCNT-FeOOH.

Similar mechanism have been proposed by several researchers when exploring As(III) sorption onto different iron oxide based materials such as iron oxide coated multiwall carbon nanotubes (Addo Ntim and Mitra 2011), waste metal (hydr)oxide (Escudero et al. 2009), lepidocrocite (Wang and Giammar 2015), a mixture of minerals from an aquifer with high iron content (Carrillo and Drever 1998), and core-shell $Fe@Fe_2O_3$ nanobunches (Tang et al. 2017).

4. Conclusions

A novel hybrid filter for As(III) removal from water was successfully developed by surface modification of a commercial non-woven PP fabric with MWCNTs and its subsequent decoration with iron oxy(hydroxide) nanoparticles in form of akaganeite (β-FeOOH).
A Box–Behnken experimental design was successfully used to explore the effect of the initial As(III) concentration, pH and sorbent dose on As(III) removal. A cubic equation was found to provide the best description of the observed sorption behavior.
The removal of As(III) by the iron oxy(hydroxide)-modified material is mainly based on the linkage of neutral H_3AsO_3 moieties to the free hydroxyl groups provided by the β-FeOOH with subsequent H_2O loss.

Acknowledgements

Dr. Artur Małolepszy is acknowledged for the purification of MWCNTs. This work has been supported by the European Union in the framework of European Social Fund through the Warsaw University of Technology Development Programme. This work was supported by Switzerland through the Swiss Contribution to the enlarged European Union within the project ‘‘Novel nanocomposite filter media for adsorption based water treatment – NANOSORP’’, PSP:209/2010.

References

Abernathy CO, Calderon RL, Chappell WR (1997) Arsenic; exposure and health effects doi:10.1007/978-94-011-5864-0

Addo Ntim S, Mitra S (2011) Removal of Trace Arsenic To Meet Drinking Water Standards Using Iron Oxide Coated Multiwall Carbon Nanotubes Journal of Chemical & Engineering Data 56:2077-2083 doi:10.1021/je1010664

Amini M et al. (2008) Statistical modeling of global geogenic arsenic contamination in groundwater. Environmental science & technology 42:3669-3675

Bashir S, McCabe RW, Boxall C, Leaver MS, Mobbs D (2009) Synthesis of α- and β-FeOOH iron oxide nanoparticles in non-ionic surfactant medium Journal of Nanoparticle Research 11:701-706 doi:10.1007/s11051-008-9467-z

Behzadi M, Taher MA, Hassani Moghaddam F (2017) Evaluation of the effectiveness of carbonaceous adsorbents on simultaneous extraction of heavy metals: a comparative study International Journal of Environmental Science and Technology 14:999-1010 doi:10.1007/s13762-016-1205-y

Bhatia M, Satish Babu R, Sonawane SH, Gogate PR, Girdhar A, Reddy ER, Pola M (2017) Application of nanoadsorbents for removal of lead from water International Journal of Environmental Science and Technology 14:1135-1154 doi:10.1007/s13762-016-1198-6

Carrillo A, Drever JI (1998) Adsorption of arsenic by natural aquifer material in the San Antonio-El Triunfo mining area, Baja California, Mexico Environmental Geology 35:251-257 doi:10.1007/s002540050311

Chen B et al. (2014) One-pot , solid-phase synthesis of magnetic multiwalled carbon nanotube / iron oxide composites and their application in arsenic removal JOURNAL OF COLLOID AND INTERFACE SCIENCE 434:9-17 doi:10.1016/j.jcis.2014.07.046

Escudero C, Fiol N, Villaescusa I, Bollinger J-c (2009) Arsenic removal by a waste metal (hydr) oxide entrapped into calcium alginate beads Journal of Hazardous Materials 164:533-541 doi:10.1016/j.jhazmat.2008.08.042

Ghasemzadeh G, Momenpour M, Omidi F, Hosseini MR, Ahani M, Barzegari A (2014) Applications of nanomaterials in water treatment and environmental remediation Frontiers of Environmental Science {&} Engineering 8:471-482 doi:10.1007/s11783-014-0654-0

Grant IJ, Ward IM (1965) The infra-red spectrum of syndiotactic polypropylene Polymer 6:223-230 doi:http://dx.doi.org/10.1016/0032-3861(65)90090-X

Habuda-Stanić M, Nujić M (2015) Arsenic removal by nanoparticles: a review Environmental Science and Pollution Research 22:8094-8123 doi:10.1007/s11356-015-4307-z

Holl WH (2010) Mechanisms of arsenic removal from water. Environmental geochemistry and health 32:287-290 doi:10.1007/s10653-010-9307-9
Hristovski K, Baumgardner A, Westerhoff P (2007) Selecting metal oxide nanomaterials for arsenic removal in fixed bed columns: From nanopowders to aggregated nanoparticle media Journal of Hazardous Materials 147:265-274 doi:10.1016/j.jhazmat.2007.01.017
Hu J, Tong Z, Chen G, Zhan X, Hu Z (2014) Adsorption of roxarsone by iron (hydr)oxide-modified multiwalled carbon nanotubes from aqueous solution and its mechanisms International Journal of Environmental Science and Technology 11:785-794 doi:10.1007/s13762-013-0261-9
Jamrozik A et al. (2014) Influence of iron contaminations on local and bulk magnetic properties of nonfunctionalized and functionalized multi-wall carbon nanotubes Physica Status Solidi A 669:661-669
Kim J, Van der Bruggen B (2010) The use of nanoparticles in polymeric and ceramic membrane structures: Review of manufacturing procedures and performance improvement for water treatment Environmental Pollution 158:2335-2349 doi:http://dx.doi.org/10.1016/j.envpol.2010.03.024
Kousha M, Daneshvar E, Sohrabi MS, Jokar M, Bhatnagar A (2012) Adsorption of acid orange II dye by raw and chemically modified brown macroalga Stoechospermum marginatum Chemical Engineering Journal 192:67-76 doi:10.1016/j.cej.2012.03.057
Ma J et al. (2013) One-pot, large scale synthesis of magnetic activated carbon nanotubes and their application for arsenic removal Journal of Materials Chemistry A:4662-4666 doi:10.1039/c3ta10329c
Mandal BK, Suzuki KT (2002) Arsenic round the world: a review. Talanta 58:201-235
Mishra AK, Ramaprabhu S (2010) Magnetite Decorated Multiwalled Carbon Nanotube Based Supercapacitor for Arsenic Removal and Desalination of Seawater Journal of Physical Chemistry A:2583-2590
Moradlou O, Dehghanpour Farashah S, Masumian F, Banazadeh A (2016) Magnetite nanoplates decorated on anodized aluminum oxide nanofibers as a novel adsorbent for efficient removal of As(III) vol 13. doi:10.1007/s13762-016-0941-3
Narayan R (2010) Use of nanomaterials in water purification Materials Today 13:44-46 doi:http://dx.doi.org/10.1016/S1369-7021(10)70108-5
Przekop R, Gradoń L (2008) Deposition and Filtration of Nanoparticles in the Composites of Nano- and Microsized Fibers Aerosol Science and Technology 42:483-493
Qu X, Alvarez PJJ, Li Q (2013) Applications of nanotechnology in water and wastewater treatment Water Research 47:3931-3946 doi:http://dx.doi.org/10.1016/j.watres.2012.09.058
Rosca ID, Watari F, Uo M, Akasaka T (2005) Oxidation of multiwalled carbon nanotubes by nitric acid Carbon 43:3124-3131 doi:http://dx.doi.org/10.1016/j.carbon.2005.06.019
Rossi RJ (2010) Applied Biostatistics for the Health Sciences:664
Sano E, Akiba E (2014) Electromagnetic absorbing materials using nonwoven fabrics coated with multi-walled carbon nanotubes Carbon 78:463-468 doi:http://dx.doi.org/10.1016/j.carbon.2014.07.027
Sayed M, Burham N (2017) Removal of cadmium (II) from aqueous solution and natural water samples using polyurethane foam/organobentonite/iron oxide nanocomposite adsorbent International Journal of Environmental Science and Technology doi:10.1007/s13762-017-1369-0
Shak KPY, Wu TY (2015) Optimized use of alum together with unmodified Cassia obtusifolia seed gum as a coagulant aid in treatment of palm oil mill effluent under natural pH of wastewater Industrial Crops and Products 76:1169-1178 doi:http://dx.doi.org/10.1016/j.indcrop.2015.07.072
Shokati Poursani A, Nilchi A, Hassani A, Tabibian S, Asad Amraji L (2017) Synthesis of nano-γ-Al2O3/chitosan beads (AlCBs) and continuous heavy metals removal from liquid solution International Journal of Environmental Science and Technology 14:1459-1468 doi:10.1007/s13762-017-1357-4
Smedley PL, Kinniburgh DG (2002) A review of the source, behaviour and distribution of arsenic in natural waters Applied Geochemistry 17:517-568
Sperlich A, Werner A, Genz A, Amy G, Worch E, Jekel M (2005) Breakthrough behavior of granular ferric hydroxide (GFH) fixed-bed adsorption filters: Modeling and experimental approaches Water Research 39:1190-1198
Tang L et al. (2017) Treatment of arsenic in acid wastewater and river sediment by Fe@Fe2O3 nanobunches: The effect of environmental conditions and reaction mechanism Water Research 117:175-186 doi:http://dx.doi.org/10.1016/j.watres.2017.03.059
Tawabini BS, Al-Khaldi SF, Khaled MM, Atieh Ma (2011) Removal of arsenic from water by iron oxide nanoparticles impregnated on carbon nanotubes. Journal of environmental science and health Part A, Toxic/hazardous substances & environmental engineering 46:215-223
Teh CY, Budiman PM, Shak KPY, Wu TY (2016) Recent Advancement of Coagulation–Flocculation and Its Application in Wastewater Treatment Industrial & Engineering Chemistry Research 55:4363-4389 doi:10.1021/acs.iecr.5b04703

Teh CY, Wu TY, Juan JC (2017) An application of ultrasound technology in synthesis of titania-based photocatalyst for degrading pollutant Chemical Engineering Journal 317:586-612 doi:http://dx.doi.org/10.1016/j.cej.2017.01.001
Wang L, Giammar DE (2015) Effects of pH, dissolved oxygen, and aqueous ferrous iron on the adsorption of arsenic to lepidocrocite Journal of Colloid and Interface Science 448:331-338 doi:http://dx.doi.org/10.1016/j.jcis.2015.02.047
World Health Organization WH (2008) Guidelines for drinking-water quality I:515
Żywczyk Ł, Moskal A, Gradoń L (2015) Numerical simulation of deep-bed water filtration Separation and Purification Technology 156:51-60 doi:http://dx.doi.org/10.1016/j.seppur.2015.10.003